Graded-index ridge surface plasmon polaritons waveguide

Chunwei Ye (叶春伟)[1], Yumin Liu (刘玉敏)[1,2*], Jie Wang (汪 洁)[1], Hongbo Lv (吕宏博)[1], and Zhongyuan Yu (俞重远)[1]

[1]State Key Laboratory of Information Photonics and Optical Communications, Beijing University of Posts and Telecommunications, Beijing 100876, China

[2]State Key Laboratory of Integrated Optoelectronics, Institute of Semiconductors, Chinese Academy of Sciences, Beijing 100083, China

[*]Corresponding author: microliuyumin@hotmail.com

Received March 24, 2014; accepted June 11, 2014; posted online August 27, 2014

We propose and analyze a long-range dielectric-loaded surface plasmon polariton (SPP) waveguide based on graded-index ridge over server millimeter distances. Then the influence of the dielectric thickness and the ridge refractive index on propagation length and mode width is discussed and simulated with the finite element method. The result shows that the SPP can propagate as long as 3.42 mm, as well as the mode width keeping as 1.64 μm, a better one compared with the fixed refractive index. Considering its nanoscale dimension and outstanding performance, the structure is easily realized when connected with electrodes.

OCIS codes: 240.6680, 160.4236, 230.7370.

doi: 10.3788/COL201412.092402.

Surface plasmon polariton (SPP) is a specific electromagnetic wave mode propagating along the surface of a metal as the electromagnetic wave coupled to electric oscillations[1–3]. Several waveguiding configurations, including metallic nanowires and stripes[4], metallic taper[5], wedge and grooves on a metal[6,7], support SPP modes confined laterally below the diffraction limit, which can be excited through the prism coupling, special waveguide structure, grating coupling, a strong focused beam, near-field excitation, and far-field excitation[8]. But most of them are propagating along the surface between metal and dielectric with large loss, which limit the propagation length of SPP. To solve the problem of tradeoff between confinement and loss, a ratio of the power distribution in the metal region compared to the total power of the waveguide $\mathrm{ROP}_{\mathrm{metal}}$ is introduced[9]. Moreover, a new structure called symmetric hybrid plasmonic waveguide (SHPW) has been introduced[10], by employing the strong hybridization between plasmonic and dielectric modes and optimizing the structure can result in small propagation loss, leading to a propagation distance exceeding the centimeter range, while the corresponding mode area can still be maintained within the subwavelength scale. In view of the requirement of a long propagation length as well as a strong mode confinement, more new configurations were put forward and were researched.

Long-range dielectric-loaded SPP waveguide (LR-DRSPPW)[11], whose metal film embedded in the dielectric material, has been proposed and researched in recent years. SPPs propagate along the surface between the dielectric and the nanometer-thin metal films which are sandwiched between two different dielectric materials. The LR-DRSPPW can support a SPP mode with a long propagation length as well as strong mode confinement after the geometry parameters optimization, as the works of Holmgaard[10], which can be utilized in photonic components to combine large operational bandwidth of photonics with high-density integration achievable in plasmonics[12–14].

Graded-index (GRIN) material is commonly used in fiber, usually called self-focusing optical fiber, whose core has a refractive index that decreases with increasing radial distance from the optical axis of the fiber. A GRIN square ridge of the structure is proposed and researched here. So far, the main methods of making GRIN film using physical vapor deposition are multi-source co-evaporation and single-source evaporation. When using dual-source co-evaporation and the deposition rate of SiO_2 and TiO_2 as 1:2, we can get the desired GRIN film. A structure with a GRIN square ridge is simulated here, and a longer propagation in the premise of a same mode width is achieved. In our work, the propagation length is extended by 10%, as long as 3.42 mm in a mode width of 1.42 μm.

The considered structure consists of, in the order of top to bottom, a plat and narrow metal film, sandwiched between a GRIN dielectric square ridge and a dielectric buffer layer deposited directly on a low refractive index substrate, as shown in Fig. 1. The design of substrate can limit the mode distribution area and see to that it can only exist in the region between the square ridge and buffer layer. The square ridge has been processed by filling gradient color as in Fig. 1, which represents that the refractive index of the ridge is not a constant value, conversely, descending gradually from top to bottom.

In the simulations presented below the dimension of the square ridge is 850 × 850 (nm), the bottom of which buried a 15-nm-thick and 500-nm-wide

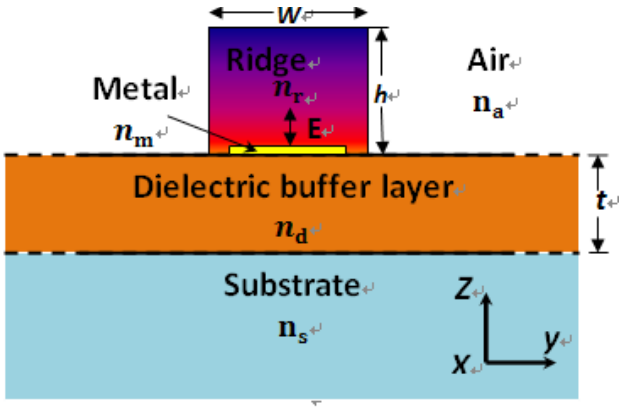

Fig. 1. Layout of the LR-DLSPPW structure, with a dielectric ridge on top of a thin metal stripe deposited on an underlying dielectric buffer layer, supported by a low-index glass substrate.

gold stripe (n_m=0.55+11.5i). Poly-methyl-methacrylate (PMMA) was chosen as the material of dielectric buffer layer (n_d=1.493), whose width was debugged to balance the mode field on either side of the metal stripe. On the bottom of the whole configurations lies a Cytop substrate, whose refractive index is n_s=1.34. In the work of Holmgaard[10] the square ridge is isotropic and homogeneous. However we have processed the ridge with special fabrication, making the refractive index descending from top to bottom. One way to manufacture such kind of elements is to use an ion diffusion process (ion exchange), and another method to realize a GRIN medium is the nonlinear optic approach[14].

The GRIN configuration is analyzed in the radio frequency (RF) section of COMSOL, which is the latest version of the software. A two-dimensional model is created and simulated at the telecom wavelength of 1.55 μm[15]. Propagation length of SPP wavelength propagating along the surface of metal and the mode width of it is calculated and drafted below. Usually, we study the imaginary part of the effective refractive index of the mode Im(n_{eff}), which is in charge of the mode damping or amplification, then obtain the propagation length

$$L = \frac{\lambda}{\left[4\pi \mathrm{Im}(n_{eff})\right]}. \quad (1)$$

As we all know, the loss of the electromagnetic wave propagating in a metal is bigger than that in a dielectric. In order to minimize the propagation losses, the mode field on either side of the metal strip must be balanced, for example, adjusting the thickness of PMMA buffer layer. Due to thin metal film, the SPPs on the two metal–dielectric interfaces couple to each other and form supermodes with symmetric and anti-symmetric transverse component (E_z)[16]. Generally, we consider the symmetric mode as the long-range mode. We can call it LR-DLSPPW, which can be considered as a hybrid of the two concepts: LRSPP and DLSPPWs. LRSPP waveguide has an mm-long propagation but poor mode confinement. In contrast, the DLSPPW has a strong mode confinement but short (~50-μm long) propagation[17]. The structure we adopted here is LR-DLSPPW. When the ridge is homogeneous and isotropic, the distribution of E_z is as shown in Fig. 2(b). The index of the square ridge ranges evenly from 1.535 to 1.62, as shown in Fig. 2(a). From the mode distribution (Fig. 2), we can find that the confinement (Fig. 2(a)) is as strong as that in Fig. 2(b) when both of them come to the optimal result.

Figure 3 shows the propagation length of four structures with different square ridge indexes. The black curve represents a structure with constant square index n_r =1.535, and the color curves represent the structures whose ridge indexes are gradient. The blue curve represents the structure with ridge index range from 1.535 to 1.5775. The red curve represents the ridge index range from 1.535 to 1.603, and the green one represents the ridge index range from 1.535 to 1.62. We can find that if the ridge index retains a constant 1.535, there will be a local maximum of 3.07 mm in the location of the PMMA thickness of 460 nm. But if the index of square is variable the location of local maximum of the propagation length moves

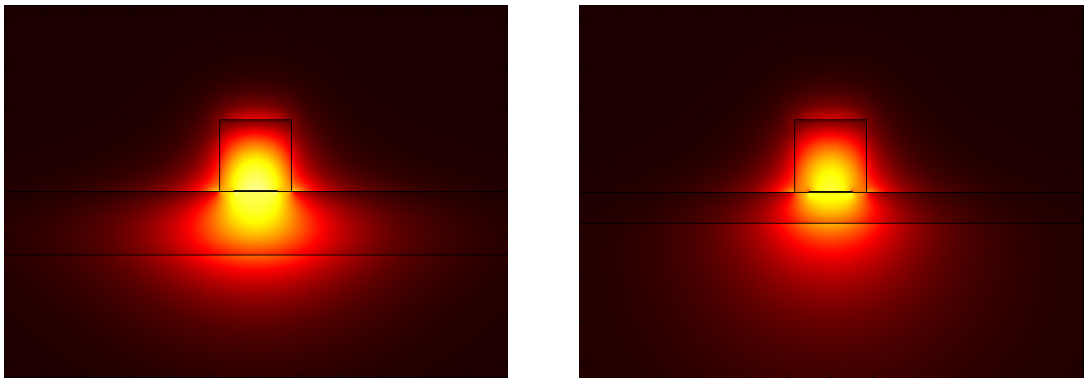

(a) (b)

Fig. 2. Field distribution of abs. (E_z) in the cross-section of the LR-DLSPPW with the parameters h = 850 nm, w = 850 nm, and (a) the index of the square ridge ranges from 1.535 to 1.62 and (b) the index of the square ridge is the constant value 1.535.

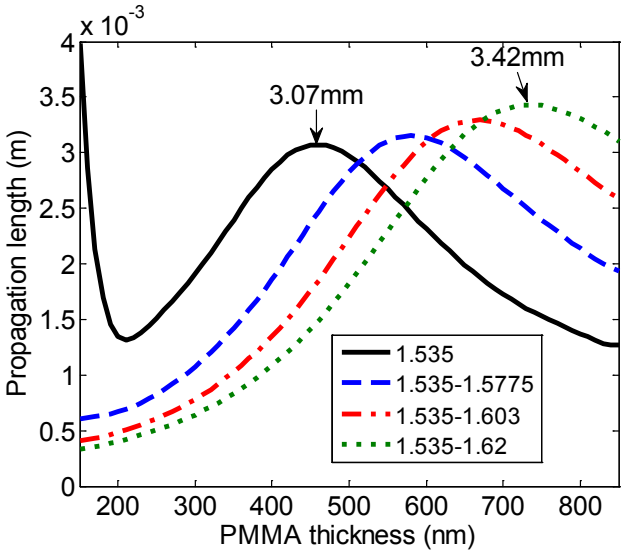

Fig. 3. Propagation length versus thickness of the PMMA buffer layer for four different graded indexes of the square ridge.

from left to right, the maximum of propagation length, of cause, becoming larger. For a greater range of variation, square index changing from 1.535 to 1.5775 (small change), the maximum of propagation is about 3.13 mm, and the corresponding PMMA buffer layer thickness is 580 nm. For an even greater range of variation, square index changing from 1.535 to 1.60 (medium change), the maximum of propagation is about 3.28 mm, and the corresponding PMMA buffer layer thickness is 680 nm. When the index of square ridge range from 1.535 to 1.62, the maximum of propagation length is up to 3.42 mm, 11.4% bigger than 3.07 mm, and the corresponding PMMA buffer layer thickness is 730 nm. This implies that increasing the index of the square ridge causes a longer propagation length.

We usually use two different methods when considering the mode field confinement of the presented structure. One is lateral mode width which determines the minimum bend radius achievable without introducing large bend losses. The other one, so-called mode area, is defined as the area encompassing half the mode energy[18]. The result of mode area can be compared directly with other plasmonic waveguides and the potential of the waveguide structure can be demonstrated. We can obtain it by taking the width of the norm of the electric field at $1/e$ of its maximum value, for more details the reader can refer to Lal *et al.*[12]. The normalized mode area is expressed by the formula $A = A_{\text{eff}}/A_0$, where $A_0 = \lambda^2/4$ is the diffraction-limited mode area, and the effective mode area A_{eff} is defined as[19]

$$A_{\text{eff}} = \frac{w_m}{\max\{W(x,y)\}} = \frac{\int\int_{-\infty}^{\infty} W(x,y)\mathrm{d}x\mathrm{d}y}{\max\{W(x,y)\}}. \quad (2)$$

Figure 4 shows the mode width versus thickness of the PMMA buffer layer for the ridge dimensions h=850 nm and w=850 nm. Figure 4(a) corresponds to the structure with a GRIN square ridge, and Fig. 4(b) corresponds to the structure with a constant-index square ridge. The insets show $E_n(y)$ at $t = 750$ nm and $t = 460$ nm, respectively. It shows the mode width falling rapidly when the PMMA thickness increases from 100 to 300 nm in Fig. 4, responding to a small PMMA thickness, for the mode starts to spread in the Cytop substrate. We can observe from Fig. 4(b) that the minimum of the mode width at t =400 nm is about 1.64 μm[12], and the curve states a slight change when it moves from 300 to 600 nm.

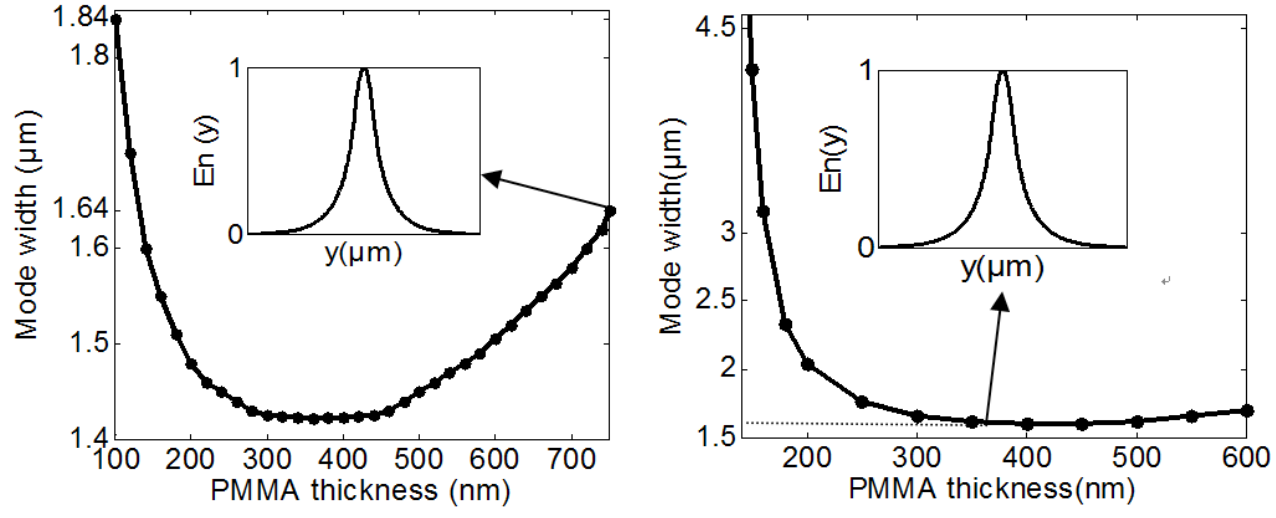

(a) (b)

Fig. 4. (a) Mode width versus thickness of the PMMA buffer layer for the GRIN ridge dimensions $h = 850$ nm, $w = 850$ nm. The inset shows $E_n(y)$ at $t = 750$ nm. (b) Mode width versus thickness of the PMMA buffer layer for a constant refractive index ridge dimensions $h = 850$ nm, $w = 850$ nm. The inset shows $E_n(y)$ at $t = 460$ nm.

A different trend is shown when the PMMA thickness moves from 300 to 600 nm (Fig. 4(a)). The minimum of the mode width is just as small as 1.42 μm, 0.22 μm lower than that in Fig. 4(b), and remain unchanging when the PMMA thickness ranges from 300 to ~ 450 nm. Although a significant increase appears when the PMMA thickness increases from 450 to 750 nm, the mode width is still 1.64 μm. As we know, when it has a maximum propagation length (3.1 mm) at $t = 460$ nm, the correspondin mode width comes to 1.64 μm[12].

From the above, it is observed that the GRIN can increase the propagation length obviously in the context of remaining in a same mode width. With its long propagation and strong confinement, a variety of integrated optical devices based on surface plasmon waveguides, such as switches[19], optical attenuators[20], modulators[21], and Bragg gratings[22], have been demonstrated. However, there still exist some limitations needed to be broken, for example, the fabrication of GRIN ridge.

In conclusion, an optimized long-range waveguide configuration based on DLSPPW with a GRIN square ridge is simulated and analyzed using COMSOL at telecom wavelengths. We obtain a large propagation length as well as retain a strong mode confinement after a series of optimization, and a longer propagation length of 3.4 mm and a smaller lateral mode width of 1.42 μm is calculated and demonstrated. The propagation length of GRIN structure promotes as long as about 11% than that of constant-index ridge. A mode guide without increasing its size has a potential of being photonic components with a high integration density and fabricating with standard lithography techniques. Another notable aspect of this configuration is its compatibility with external electrodes, which provides a favorable condition for application in designing plasmonic components.

This work was supported by the National Natural Science Foundation of China (Nos. 61275201 and 61372037), the Beijing Excellent Ph.D. Thesis Guidance Foundation (No. 20131001301), the Fund of State Key Laboratory of Information Photonics and Optical Communications (Beijing University of Posts and Telecommunications), and the Opened Fund of the State Key Laboratory on Integrated Optoelectronics, Institute of Semiconductors, Chinese Academy of Sciences.

References

1. L. Novotny and B. Hecht, *Principles of Nano-optics* (Cambridge University Press, Cambridge, 2006).
2. S. Pandey, S. Liu, B. Gupta, and A. Nahata, Photon. Res. **1,** 148 (2013).
3. W. M. Wang, Z. M. Sheng, Y. T. Li, and J. Zhang, High Power Laser Sci. Eng. **1,** 74 (2013).
4. J. Takahara, S. Yamagishi, H. Taki, A. Morimoto, and T. Kobayashi, Opt. Lett. **22,** 475 (1997).
5. C. L. Wang and C. S. Tsai, J. Lightwave Technol. **15,** 1708 (1997).
6. H. S. Yang, J. Ma, and Z. Z. Lu, IEEE Trans. Microwave Theory Tech. **43,** 324 (1995).
7. X. Li, Q. Tan, and B. Bai, Chin. Opt. Lett. **10,** 052401 (2012).
8. W. L. Barnes, A. Dereux, and T. W. Ebbesen, Nature **424,** 824 (2003).
9. H. Yin, Y. Liu, and Z. Yu, Chin. Opt. Lett. **11,** 101901 (2013).
10. T. Holmgaard, J. Gosciniak, and S. I. Bozhevolnyi, Opt. Express **18,** 23009 (2010).
11. D. K. Gramotnev and S. I. Bozhevolnyi, Nat. Photon. **4,** 83 (2010).
12. S. Lal, S. Link, and N. J. Halas, Nat. Photon. **1,** 641 (2007).
13. H. Kurt, in *Proceedings of 13th IEEE International Conference on Transparent Optical Networks* (ICTON *2011*) 1 (2011).
14. J. J. Burke, G. I. Stegeman, and T. Tamir, Phys. Rev. B **33,** 5186 (1986).
15. J. Gosciniak, T. Holmgaard, and S. I. Bozhevolnyi, J. Lightwave Technol. **29,** 1473 (2011).
16 R. F. Oulton, G. Bartal, D. F. P. Pile, and X. Zhang, New J. Phys. **10,** 105018 (2008).
17. G. Gagnon, N. Lahoud, G. A. Mattiussi, and P. Berini, J. Lightwave Technol. **24,** 4391 (2006).
18. S. Park and S. H. Song, Electron. Lett. **42,** 402 (2006).
19. Y. Ma, G. Farrell, Y. Semenova, and Q. Wu, Opt. Lett. **39,** 973 (2014).
20. T. Nikolajsen, K. Leosson, and S. I. Bozhevolnyi, Appl. Phys. Lett. **85,** 5833 (2004).
21. S. Jetté-Charbonneau, R. Charbonneau, N. Lahoud, G. Mattiussi, and P. Berini, Opt. Express **13,** 4674 (2005).
22. Y. Bian and Q. Gong, J. Opt. **16,** 015001 (2014).